Journal of Computational Electronics 2: 491–495, 2003
© 2003 Kluwer Academic Publishers. *Manufactured in The Netherlands.*

A Quantum Correction Model for Nanoscale Double-Gate MOS Devices Under Inversion Conditions

YIMING LI*
Department of Nano Device Technology, National Nano Device Laboratories, Hsinchu 300, Taiwan; Microelectronics and Information Systems Research Center, National Chiao Tung University, Hsinchu 300, Taiwan
ymli@mail.nctu.edu.tw

TING-WEI TANG
Department of Electrical and Computer Engineering, University of Massachusetts, Amherst, MA 01003, USA

SHAO-MING YU
Department of Computer and Information Science, National Chiao Tung University, Hsinchu 300, Taiwan

Abstract. A quantum correction model for nanoscale double-gate MOSFETs under inversion conditions is proposed. Based on the solution of Schrödinger-Poisson equations, the developed quantum correction model is optimized with respect to (i) the left and right positions of the charge concentration peak, (ii) the maximum of the charge concentration, (iii) the total inversion charge sheet density, and (iv) the average inversion charge depth, respectively. This model can predict inversion layer electron density for various oxide thicknesses, silicon film thicknesses, and applied voltages. Compared to the Schrödinger-Poisson results, our model prediction is within 3.0% of accuracy. This quantum correction model has continuous derivatives and is therefore amenable to a device simulator.

Keywords: quantum correction, double-gate MOS structure, inversion condition

1. Introduction

Double-gate (DG) MOSFET is attracting more and more attention and is considered as a basic structure for achieving the ultimate silicon devices in recent years [1–6]. As the feature size of the DG MOS devices is further scaled into a nanoscale regime, it has become necessary to consider quantum mechanical effects when performing device modeling. For the oxide thickness (T_{ox}) of 1–3 nm, the thickness of silicon film (T_{si}) of 2–20 nm, and the applied gate voltage (V_G) of 0.5–1.5 volts, the inversion carrier density in the DG MOS structure shifts away from both the S_iO_2/S_i interfaces due to the quantization effect. Thus any accurate calculation of the inversion-layer charge must take this quantization effect into consideration. The most accurate way of incorporating the quantum effect in the inversion layer is to solve the coupled Schrödinger-Poisson (SP) equations subject to an appropriate boundary condition at both the S_i/S_iO_2 interfaces [7]. This can be done without difficulties in solving the SP equations in one-dimension (1D), but the SP approach is not amenable to a realistic device simulator such as a simple quantum correction model. Other approaches, for example, the density gradient method [8,9] and the effective potential method [10,11] also suffer from the same disadvantage—computationally it is still excessive, and physically the method is not very transparent.

In this paper, based on our recent work [12], we have successfully developed a new quantum correction

*To whom correspondence should be addressed.

model feasible for nanoscale DG MOS devices under inversion conditions. The solution of SP equations is utilized to construct the model, where four physical-based optimization constraints: (i) the left and right positions of the charge concentration peak, (ii) the maximum of the charge concentration, (iii) the total inversion charge sheet density Q, and (iv) the average inversion charge depth $\langle x \rangle$ are used as criteria for the model parameter formulation. The model parameters are function of T_{ox}, T_{si}, and V_G; for other applications, they can be also expressed in terms of the surface electric field, the thickness of silicon film, and the oxide thickness.

2. Model Construction

Firstly, a poly1- S_iO_2-S_i-S_iO_2-poly2 system as shown in Fig. 1 is simulated using the drift-diffusion (DD) approximation. The DD equations are solved self-consistently with the SP equations. The SP equations are assumed to have no wave penetration at both the Si/SiO_2 interfaces. More than thirty-two sub-bands are computed in the Schrödinger equation solver [13,14]. Under the inversion condition for both the symmetric and asymmetric cases, it is sufficient to consider the electron density from the left interface of S_iO_2/S_i to half silicon film $\xi_0 = T_{si}/2\lambda_{th}$. The inversion-layer charge densities are

$$n_{QM} = n_{CL}a_0\left[1-\exp\left(-a_1\xi^2\left(1+\frac{1}{4}\left(\frac{\xi}{\xi_0}\right)^2\right)\right)\right], \quad (1)$$

where n_{CL} is the classical electron density solved from the Poisson equation, $\xi = x/\lambda_{th}$, and $\lambda_{th} = (\frac{\hbar^2}{2m^* k_B T})^{1/2}$ is the thermal wavelength. Using a generic algorithm

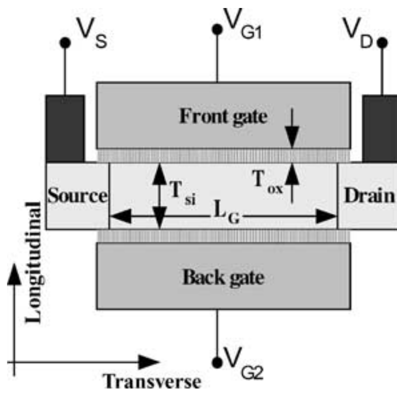

Figure 1. A cross section view of the nanoscale DG MOSFET.

[15], the two model parameters a_0 and a_1 are optimized to best fit the self-consistent SP solution for all T_{ox}'s, T_{si}'s, and V_G's cases. The accuracy of these parameters is based on the optimization with respect to the aforementioned four physical constraints. The average inversion charge depth $\langle x \rangle = \int_0 xn(x)dx/\int_0 n(x)dx$. The chosen T_{ox} varies from 1 nm to 3 nm, T_{si} varies from 5 nm to 20 nm, and the applied V_G ranges from 0.5 to 1.5 V. For example, the results of these two parameters a_1 and a_2 for the symmetric case with $T_{ox} = 2$ nm are shown in Figs. 2(a) and (b). For the asymmetric case when $V_{G2} = 1$ V is fixed the two model parameters a_0 and a_1 are shown in Figs. 2(c) and (d). After optimization, these two parameters for both the symmetric and asymmetric cases are functions of T_{ox}, T_{si}, and V_G:

$$a_0 = 2.506 - 0.077T_{ox} - 0.0427T_{si} + (0.332 + 0.0082T_{ox})\left(\frac{V_{G1}+V_{G2}}{2}\right), \quad (2)$$

$$a_1 = \frac{f(V_{G1}) - f(V_{G2})}{2} \times \frac{V_{G1}}{V_{G1}+V_{G2}} + f(V_{G1}), \quad (3)$$

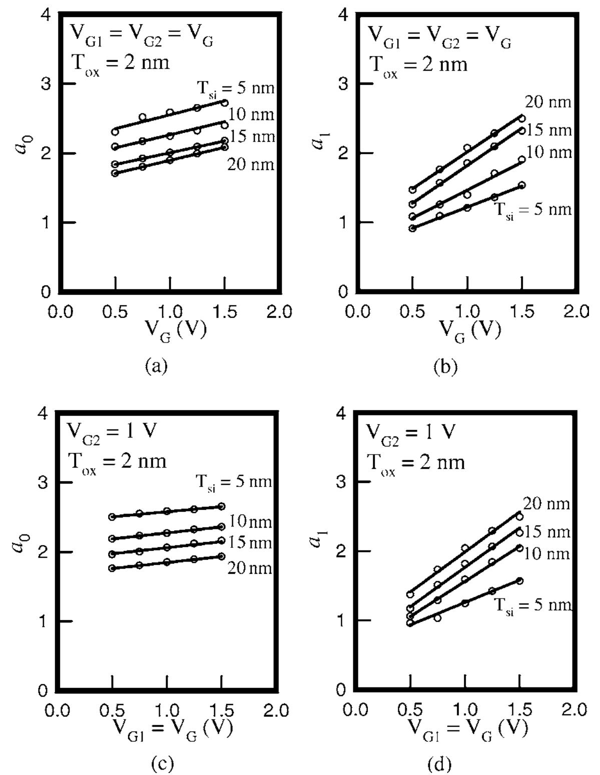

Figure 2. Plots of the optimal value for the parameters (a) a_0 and (b) a_1 and their formulas for a symmetric case with various T_{si} and different V_G, where $T_{ox} = 2$ nm. (c) and (d) are asymmetric cases.

where $f(V_G) = 1.921 + 0.0479T_{\text{ox}} + 0.10002T_{\text{si}} - 0.0275T_{\text{ox}}T_{\text{si}} - 2.388\exp(-V_G)$.

The a_0 and a_1 given in Eqs. (2) and (3) are based on a p-type substrate with $N_A = 10^{17}$ cm^{-3}. V_G is in volts; T_{ox} and T_{si} are in nm. For other dopings, V_G should be adjusted by an amount equal to a shift in the threshold voltage due to the change in N_A. However, this adjustment is usually very small (~0.1 V). For other applications such as a 2D simulation, it is more convenient to express a_0 and a_1 in terms of T_{ox}, T_{si}, and the surface electric field E_s:

$$a_0 = 2.282 - 0.0487T_{\text{ox}} - 0.0640T_{\text{si}} + 5.49810^{-4}T_{\text{ox}}T_{\text{si}}^2 + 0.484\left(\frac{E_{S1} + E_{S2}}{2}\right)^{2/3}, \tag{4}$$

$$a_1 = \frac{f(E_{S1}) - f(E_{S2})}{2} \times \frac{E_{S1}}{E_{S1} + E_{S2}} + f(E_{S1}), \tag{5}$$

where $f(E_s) = -0.797 + 0.227T_{\text{ox}} + 0.0983T_{\text{si}} - 1.0194T_{\text{ox}}T_{\text{si}}^2 + 0.328\exp(E_S^{2/3})$. T_{ox} and T_{si} are in nm, and the E_s in MV/cm is self-consistently computed with the DD model.

3. Results and Discussion

The accuracy of the model inversion-layer charge density given by Eqs. (1)–(3) compared to the SP solution is very good. In terms of the four criteria mentioned above, the accuracy is within 3%. Shown in Figs. 3 and 4 are respectively electron densities for both the cases of the symmetric and asymmetric DG MOS structures with $T_{\text{ox}} = 2$ nm. Figure 3 shows the electron density at $V_{G1} = V_{G2} = V_G = 0.5$ V, where the circles are the result of our model and the lines are the SP results. Figure 4 is the electron density at $V_{G1} = 1$ V and $V_{G2} = 0.75$ V. It is found that the results of our model are in a good agreement on the SP results. Shown in Figs. 5 and 6 are respectively errors between the formulated a's formula and the SP solution against V_G for each optimization criterion. Figure 5(a) and (b) show that the error of the total inversion charge sheet density Q between our model and the SP equation is less than 3%. Figure 6(a) and (b) show that the error of the average inversion charge depth $\langle x \rangle$ is within 3%. Similarly, for both the symmetric and asymmetric cases, the errors of the left and right positions of the charge concentration peak are less than 2.5% and 2.9%, respectively. The errors of the maximum of the charge concentration are within 2% for both cases.

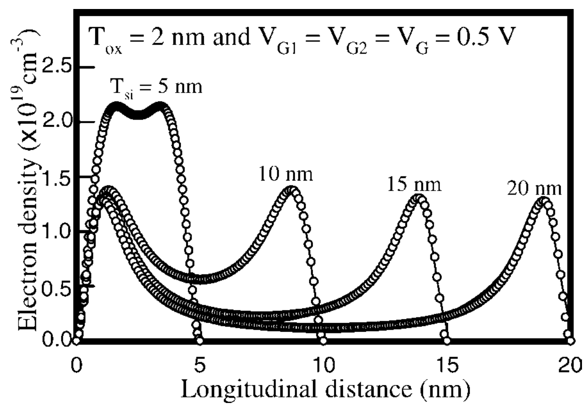

Figure 3. Plot of electron density for a symmetric DG MOS with different T_{si} where $T_{\text{ox}} = 2$ nm and $V_{G1} = V_{G2} = V_G = 0.5$ V.

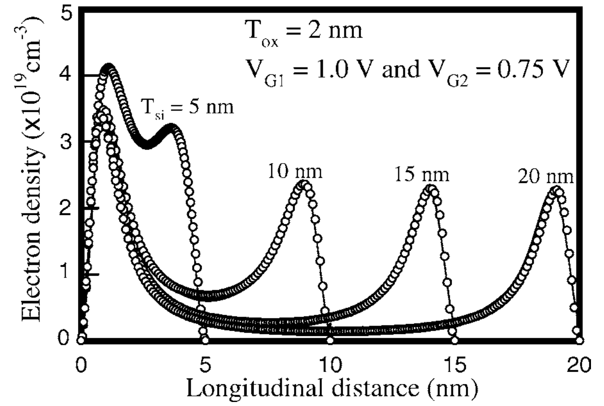

Figure 4. Plot of electron density for an asymmetric DG MOS with different T_{si} where $T_{\text{ox}} = 2$ nm, $V_{G1} = 1.0$ V, and $V_{G2} = 0.75$ V.

For the doping concentration N_A varying from 10^{16} to 10^{18} cm^{-3}, the errors versus V_G are also estimated with the same a's formula. We have found that the variations of errors are all within 3%, and this maximum error of the average inversion charge depth occurred at $N_A = 10^{16}$ cm^{-3}, $T_{\text{ox}} = 3.0$ nm, $T_{\text{si}} = 20$ nm, $V_{G1} = 1.5$ V, and $V_{G2} = 0.5$ V. For a DG MOSFET with the Gaussian and low-high-low doping profiles, we have also found that the error trend is similar to one which has the uniform doping, and the largest error fluctuation (3.2% for Gaussian doping profile) occurs at low doping level ($N_A = 10^{16}$ cm^{-3}), thicker oxide thickness ($T_{\text{ox}} = 3.0$ nm), thicker silicon film thickness ($T_{\text{si}} = 20$ nm), and asymmetric case ($V_{G1} = 1.5$ V and $V_{G2} = 0.5$ V).

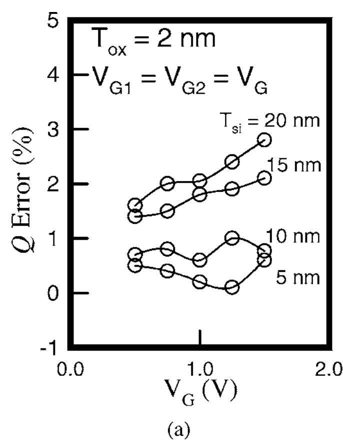

(a)

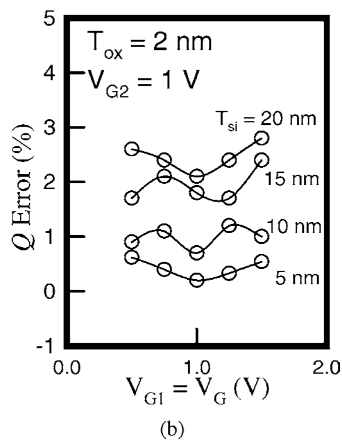

(b)

Figure 5. The error plots of the total inversion charge sheet density Q vs. V_G with respect to T_{si} for (a) symmetric and (b) asymmetric cases.

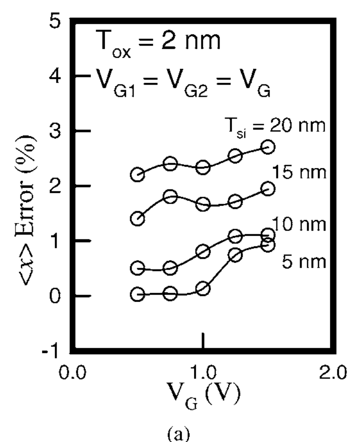

(a)

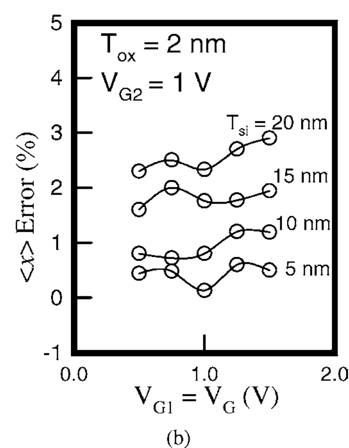

(b)

Figure 6. The error plots of the average inversion charge depth $\langle x \rangle$ vs. V_G with respect to T_{si} for (a) symmetric and (b) asymmetric cases.

4. Conclusions

Based on the SP solutions, we have developed a quantum correction model for correcting the classical inversion-layer charge distribution which agrees with the SP solution within 3%. By inputting the classical charge density from the series expansion solution of Poisson equation [16,17] or the DD based simulator together with the device oxide thickness, silicon film thickness, and gate voltage, the proposed inversion-layer charge correction model calculates nanoscale DG MOSFET inversion charge explicitly, taking into consideration of the quantum effect. This inversion-layer charge correction model has continuous derivatives and therefore is amenable to a device simulator. Due to high gate tunneling for the MOS structure with $T_{ox} < 1$ nm, it is necessary for the model to include tunneling effects at high gate voltage.

Acknowledgment

This work is supported in part by the National Science Council of TAIWAN under contract numbers: NSC-92-2112-M-429-001 and NSC-92-2815-C-492-001-E. It is also supported in part by the grant of the Ministry of Economics Affairs, Taiwan under contract No. 91-EC-17-A-07-S1-0011.

References

1. M. Masahara, T. Matsukawa, K. Ishii *et al.*, In *IEEE IEDM Tech. Dig.* (2002), p. 17_08.
2. B. Yu, L. Chang, S. Ahmed *et al.*, In *IEEE IEDM Tech. Dig.* (2002), p. 10_02.
3. G. Pei, J. Kedzierski, P. Oldiges *et al.*, *IEEE Trans. Electron Devices*, **49**, 1411 (2002).
4. C. Fiegna and A. Abramo, In *Proc. IEEE SISPAD* (1997), p. 93.

5. M. Mouis, F.-N. Genin, and A. Poncet, In *Proc. IEEE Device Research Conf.* (2001), p. 195.
6. S.E. Laux, A. Kumar, and M.V. Fischetti, In *IEEE IEDM Tech. Dig.* (2002), p. 29_04.
7. F. Stern and W.E. Howard, *Phys. Rev.*, **163**, 816 (1967).
8. M.G. Ancona, Z. Yu, R.W. Dutton *et al*., *IEEE Trans. Electron Devices*, **47**, 2310 (2000).
9. T.-W. Tang, X. Wang, and Y. Li, *J. Computational Electronics*, **1**, 389 (2002).
10. S.M. Ramey and D.K. Ferry, *Physica.*, **B314**, 350 (2002).
11. D.K. Ferry, *VLSI Design*, **13**, 155 (2001).
12. T.-W. Tang and Y. Li, *IEEE Trans. Nanotech*., **1**, 243 (2002).
13. Y. Li, T.S. Chao, and S.M. Sze, *Int. J. Modelling and Simulation*, **23**, 94 (2003).
14. Y. Li, J.W. Lee, T.-W. Tang *et al*., *Comput. Phys. Commun.*, **147**, 214 (2002).
15. Y. Li, Y.Y. Cho, C.S. Wang *et al*., *Jpn. J. Appl. Phys.*, **42**(Part 1, 4B), 2371 (2003).
16. Y. Taur and T.H. Ning, "Fundamentals of Modern VLSI Devices" (Cambridge, New York, 1998).
17. J.C.S. Woo, K.W. Terrill, and P.K. Vasudev, *IEEE Trans. Electron Devices*, **37**, 1999 (1990).